Journal of
Water & Climate Change

IWA PUBLISHING

Journal of Water and Climate Change Vol 14 No 8, 2861 doi: 10.2166/wcc.2023.217

A diverse influence of dissolved natural organic matter on light irradiance measurements in lakes

Ståle Haaland [a,b,*], Jonatan Haga[c] and Øivind Wien[d]

[a] Norwegian Institute of Bioeconomy Research, P.O. Box 115, NO-1431 Ås, Norway
[b] Norwegian University of Life Sciences, NMBU, P.O. Box 5003, NO-1432 Ås, Norway
[c] Indre Østfold, P.O. Box 34, NO-1861 Trøgstad, Norway
[d] Sweco, P.O. Box 80 Skøyen, NO-0212 Oslo, Norway
*Corresponding author. E-mail: staale.haaland@nibio.no

SH, 0009-0005-0687-4790

ABSTRACT

Light penetration plays a vital role in lakes and drinking water reservoirs, influencing fundamental processes such as primary production and thermal budgets. The Secchi depth (Z_{SD}) and the compensation depth (Z_{CD}) are commonly used measurements in this context. Z_{SD} is determined through visual inspection using a Secchi disc, while Z_{CD} represents the depth at which photosynthetic activity balances respiration and can be measured using a quantum irradiance sensor. Through *in situ* water-core samples from 23 lakes within a lake district in Southeastern Norway, we observed that DNOM exerts a diverse influence on these light irradiance measurements. If DNOM concentrations are reduced to half or a quarter of the current concentration, similar to what was measured during the 1980s, the median Z_{CD}:Z_{SD} ratios are estimated to have decreased by approximately 30 and 60% since then, respectively. Conversely, a plausible future climate-driven doubling or quadrupling of the present DNOM concentrations are estimated to further decrease the median Z_{CD}:Z_{SD} ratios in the lake district with approximately 10 and 25%, respectively. From this, the Z_{CD}:Z_{SD} ratios seem to have experienced a considerable long-term decline attributed to both climate change and the recovery from acid rain, and a further climate-driven decrease is expected.

Key words: allochthonous dissolved natural organic matter (DNOM), climate change, compensation depth (Z_{CD}), PAR-light, Secchi depth (Z_{SD}), water-core samples

HIGHLIGHTS

- A long-term DNOM decline has had a diverse impact on two classical lake irradiance measurements – Secchi depth (Z_{SD}) and compensation depth (Z_{CD}) measurements.
- Irradiance measurements are affected by parameters scattering and absorbing light.
- Z_{CD} is relatively more affected by DNOM.
- Z_{SD} is relatively more affected by turbidity.
- Z_{CD}:Z_{SD} ratios have had a long-term decrease within a lake district in Norway.

GRAPHICAL ABSTRACT

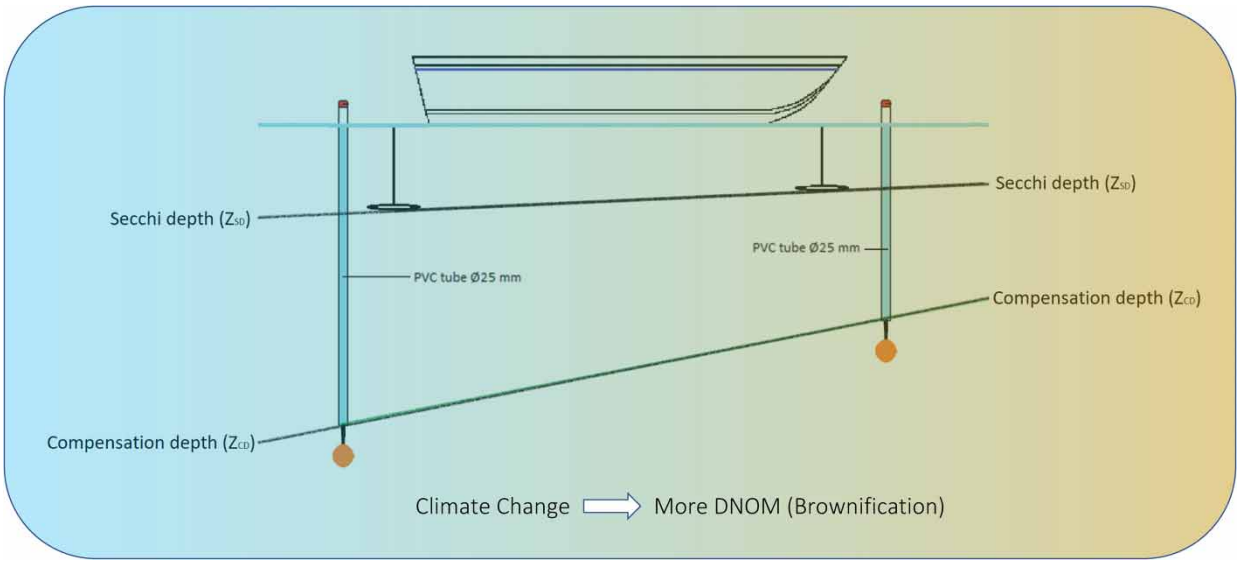

INTRODUCTION

The total scalar irradiance of solar radiation, along with the subsequent attenuation of specific wavelengths, plays a significant role in various crucial processes within lake ecosystems. The extent of light irradiance influences primary production, thermal budgets, stratification, thermocline depths, and circulation patterns (Eloranta 1978; Read & Rose 2013; Thrane *et al.* 2014; Rohrlack *et al.* 2020). When sunlight enters the lake, it encompasses a range of wavelengths, from highly energetic ultraviolet (UV) radiation to less energetic infrared light. The attenuation of photosynthetically active radiation (PAR; 400–700 nm) affects both the transparency of lake water (Secchi depth, Z_{SD}) and the depths of the euphotic zone, which extend down to the compensation depth (Z_{CD}). Z_{SD} is commonly used to measure water transparency or clarity *in situ* and is typically interpreted as the depth at which 10% of PAR-light is still present (Preisendorfer 1986). Z_{SD} is interpreted by the human eye using a submersed Secchi disc. Z_{CD} is measured using a digital quantum sensor and represents the depth at where photosynthetic activity is in balance with respiration.

The attenuation of light is caused by both scattering and absorbance, $k_{tot}(\lambda) = k_{scat}(\lambda) + k_{abs}(\lambda)$. Scattering of PAR primarily occurs due to water molecules and particulate suspended matter. Particles able to scatter light in the water phase would be of both organic (i.e., algae; organic seston) and inorganic (i.e., colloids and clay; inorganic seston) origin (Kirk 1980; Bohren & Huffman 1998). On the other hand, the absorbance of PAR is largely influenced by the absorption of water molecules (Kirk 1980, 1985), autochthonous dissolved organic matter (detritus and algae) (Kirk 2011), and allochthonous-derived dissolved organic matter (DNOM) (Kirk 1976). Since both Z_{SD} and Z_{CD} are influenced by light scattering and the absorption of light by pigment systems (Brezonic 1978), Z_{SD} is often used in various conversions to estimate Z_{CD} in lakes, which typically varies among lakes from less than 1 to greater than 5 times Z_{SD} (Smetacek & Passow 1990). Z_{SD} and Z_{CD} are, however, influenced differently by substances that attenuate PAR (Koenigs & Edmundson 1991; Luhtala & Tolvanen 2013). Z_{SD} is primarily affected by light scattering (Kirk 1985). An increase in particles and turbidity suggests an underestimation of Z_{CD} when converting from Z_{SD}. On the other hand, the vertical attenuation coefficients for irradiance are strongly influenced by the light absorption of DNOM, specifically humic matter (Kirk 1976; Branco & Kremer 2005; Kostoglidis *et al.* 2005; Urtizberea *et al.* 2013). From this, an increased concentration of DNOM might suggest an overestimation of Z_{CD} when converting from Z_{SD}.

Regarding the light absorbing and light scattering parameters in Southeastern Norwegian lakes, allochthonous produced (catchment origin) DNOM is the one parameter that has changed a lot over the past few decades (Haaland *et al.* 2010; Riise *et al.* 2018). This is mainly due to climate change and acid rain, and concurrent variations in DNOM concentrations have been observed within large boreal and hemiboreal areas (Monteith *et al.* 2007, 2023; Riise *et al.* 2018; De Wit *et al.* 2023). Allochthonous DNOM exhibits strong light absorption capabilities in the UV range and shorter wavelengths of PAR (Steinberg 2003). This absorption is attributed to the molecular orbitals in DNOMs (dissolved organic matter) and their

conjugated pigment systems (Shapiro 1957; Steinberg 2003), and also in complexation with ferrous iron in surface waters (Gjessing 1964; Poulin *et al.* 2014; Riise *et al.* 2023). Climate change is at present and in the future expected to be the most prominent driver for DNOM concentrations in European and North American lakes, including shifts in rainfall, sea-salt exposure and runoff patterns (Haaland *et al.* 2010; Weyhenmeyer *et al.* 2014; De Wit *et al.* 2016; Monteith *et al.* 2023), redox effects (Clark *et al.* 2006; Kritzberg & Ekström 2012; Monteith *et al.* 2023), temperature fluctuations (Freeman *et al.* 2001; Hytteborn *et al.* 2015; Haaland *et al.* 2018; Monteith *et al.* 2023), and due to changes in catchment properties such as vegetation cover and greening (Larsen *et al.* 2010; Finstad *et al.* 2016; Haaland *et al.* 2018). The decline in acid rain deposition in European and North American catchment soils has previously been regarded as a strong driver behind changes in DNOM concentrations over the past few decades (Forsberg & Petersen 1990; Monteith *et al.* 2023), for instance affecting changes in soil solution ionic strength (Evans *et al.* 2006; Monteith *et al.* 2007, 2023; Haaland *et al.* 2010).

Accurate assessment of light irradiance is important for understanding processes within lake ecosystems. We know that Z_{SD} is often used in various conversions for estimates of Z_{CD} in lakes, that DNOM has a diverse influence on light irradiance measurements and that DNOM concentrations have increased and is projected to increase further in concentration due to climate change. However, to which extent changes in DNOM concentration have affected the measurements of Z_{CD} and Z_{SD} differently remains unknown. From this, a sampling survey was performed in a lake district in Southeastern Norway, measuring light irradiance, well-known parameters affecting light irradiance (including DNOM), and also involving the use of integrated water-core samples.

MATERIALS AND METHODS

Site description

We utilized a dataset obtained from a lake district in Southeastern Norway (Viken County; Figure 1). The dataset involved samples from 23 dimictic lakes taken during the summer months of June and August. The lakes are situated within the

Figure 1 | The sampled lake districts are within Viken county (and within former Akershus county and Østfold county), Southeastern Norway (red area). Please refer to the online version of this paper to see this figure in colour: https://dx.doi.org/10.2166/wcc.2023.217.

latitude range of 58–60°N and longitude range of 10–12°E, with an altitude below 300 m. The selection was based on their representative water quality, encompassing a wide range of chemical compositions and concentrations of dissolved and suspended organic and inorganic compounds.

Field measurements of Z_{SD} and Z_{CD}

Water transparency, represented by the Secchi depth (Z_{SD}), was determined using a 13 × 18 cm Secchi disk and a water scope following the method described by Preisendorfer (1986). Z_{SD} was calculated as the average of one descending and one ascending measurement. Measurements of the compensation depth (Z_{CD}) were done by measuring the quantum irradiance (Q) within the PAR range until Q dropped below 0.2 μmol m^{-2} s^{-1}. Z_{CD} was determined as the depth at which 1% of downward PAR irradiance remained. A combination of a quantum sensor (LI-COR LI-192) and a light meter (LI-COR LI-250) was used for this purpose. To eliminate any potential shading effects, the quantum sensor was submerged 2 m away from the boat. If deviations between measurements exceeded 5%, the measurements were repeated from the beginning. Both measurements were carried out between 09:00 AM and 15:00 PM to minimize discrepancies caused by variations in sun altitude (Simon & Shanmugam 2013).

Integrated water-core samples

To establish a correlation between light measurements and the physical and chemical parameters influencing light absorbance and light scattering, integrated core samples were collected from the lake's surface down to the compensation depth (Z_{CD}). PVC tubes with a diameter of 25 mm and equipped with a sinker for stability (Figure 2) were used for sampling. The tube was sealed when Z_{CD} was reached. Water from the tube was transferred to a 10 L container, thoroughly mixed, and subsampled into 0.5 L bottles. These samples were stored in darkness at 4 °C until further analysis.

Measurements of parameters influencing light absorbance and light scattering

Spectrometric absorption measurements were conducted using a Perkin Elmer Lambda double-beam instrument equipped with a 50 mm quartz cuvette. The scans were conducted over 400–700 nm at a resolution of 1 nm. The absorption of DNOM was quantified at 400 nm (DNOM (m^{-1})). To establish the absorption background attributed to water molecules, reverse osmosis ultrapure water was utilized. The concentration of dissolved organic carbon (DOC) was also used as a proxy measurement for the concentrations of DNOM and was determined using a Shimadzu TOC-V total carbon analyzer.

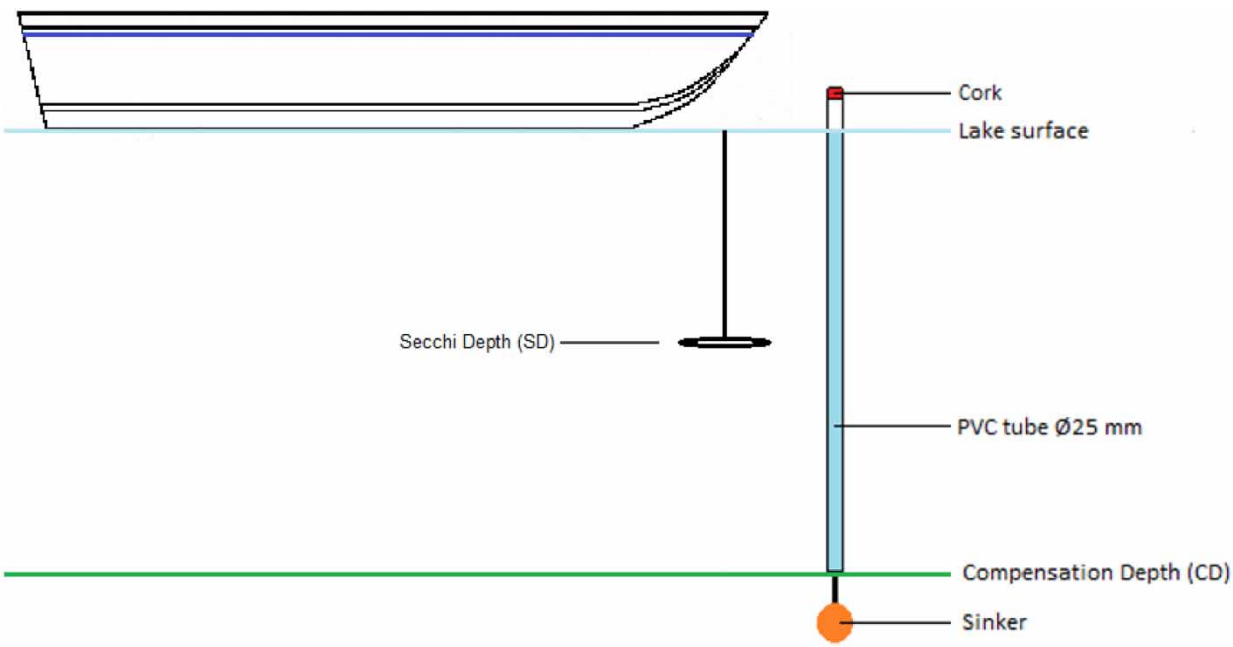

Figure 2 | Sampling set-up for integrated water-core samples. The sinker was attached for straightening out the tube. The compensation depth (Z_{CD}) was interpreted as the depth at where 1% downward PAR irradiance was left.

The dissolved carbon fraction (DOC), obtained after filtration with a 0.45 μm filter, accounted for more than 95% of the total carbon fraction (TOC). True color unit (TCU) estimates were obtained using a platinum cobalt chloride color standard. Turbidity (measured in Formazin Nephelometric Units, FNU) was assessed using a HACH 2100AN IS turbidimeter. Seston, representing suspended particles, was measured by collecting filtrates on dried (at 105 °C) Whatman GF/C filters with a median retention particle size of 1.2 μm. The filters were subsequently heated at 450 °C for 2 h to separate seston into inorganic and organic fractions. Other chemical analyses were conducted following ISO standards (as indicated in Table 1). Statistical analysis of the data was performed using R, Minitab Statistical Software, and Matlab.

RESULTS

Water quality statistics for the 23 lakes sampled in Southeastern Norway are given in Table 1. Turbidity measurements, indicating scattered light, ranged from 0.3 to 28 FNU. The concentrations of total seston varied from 0.5 to over 15 mg L^{-1}, reflecting a range from non-turbid lakes to moderately turbid lakes. Hazen color units (TCU) revealed a diversity in water color, with values below 3 mg Pt L^{-1} for clear water lakes and exceeding 100 mg Pt L^{-1} for lakes with more pronounced coloration. Notably, there was a strong linear relationship observed between allochthonous DNOM and DOC ($r^2 = 0.94$), as well as between DOC and TCU ($r^2 = 0.93$). The measurements of compensation depth (Z_{CD}) and Secchi depth (Z_{SD}) exhibited a high correlation among the lakes ($r^2 = 0.94$), as expected. However, there were variations between lakes regarding the dominant factor influencing the attenuation coefficient for photosynthetically active radiation (k_d PAR). Approximately 70% of the lakes were primarily influenced by DNOM, while suspended matter played a dominant role in the remaining lakes.

Figure 3 displays a similarity plot (dendrogram) illustrating the correlation coefficient distances between different water quality parameters obtained from the water sample cores, following the approach described by Van Sickle (1997). The plot reveals two main branches.

The first branch, cluster_a, comprises parameters such as Secchi depth (Z_{SD}) and measures related to suspended matter, including inorganic seston and turbidity. Cluster_b encompasses chemical and physical parameters like conductivity, pH,

Table 1 | Water quality statistics

Parameter (unit)	Min	Median	Average	Max
Compensation depth, Z_{CD} (m)	0.7	3.2	4.4	20.5
Secchi depth, Z_{SD} (m)	0.5	2.5	3.4	13.4
Z_{CD}:Z_{SD} ratio	0.9	1.3	1.4	2.9
$DNOM_{400}$ (m^{-1})	0.1	2.5	3.2	10.8
DOC (mg L^{-1})	0.2	6.7	7.4	18.4
TCU (mg Pt L^{-1})	3	45	50	155
k_d PAR (m^{-1})	0.2	1.4	1.8	5.4
Algal (wet, mm^3 m^{-3})*	36	189	1,049	5,816
Chl_a (μg L^{-1})	0.3	5.2	17.5	131
Turbidity (FNU)	0.3	2.2	5.0	28.0
$Seston_{org}$ (mg L^{-1})	0.4	1.3	2.3	11.6
$Seston_{inorg}$ (mg L^{-1})	0.1	1.1	2.1	15.5
$Seston_{org}$ to $Seston_{inorg}$ ratio	0.04	0.5	1.1	10.0
pH	5.2	6.9	7.0	9.8
Alkalinity (μmol_c L^{-1})	0	122	204	871
Conductivity (mS m^{-1})	6	47	66	283
TP (μg L^{-1})	3	42	72	407
TN (mg L^{-1})	0.1	0.6	21	478

Secchi depth (Z_{SD}) is the average of one descending and one ascending measure. Compensation depth (Z_{CD}) is interpreted as the depth at where 1% PAR-light is left. The specific visual light absorbance (sVISa) is calculated as DNOM (m^{-1} at 400 nm) divided by DOC (mg L^{-1}).

*20 of the 23 lakes did have an algal count.

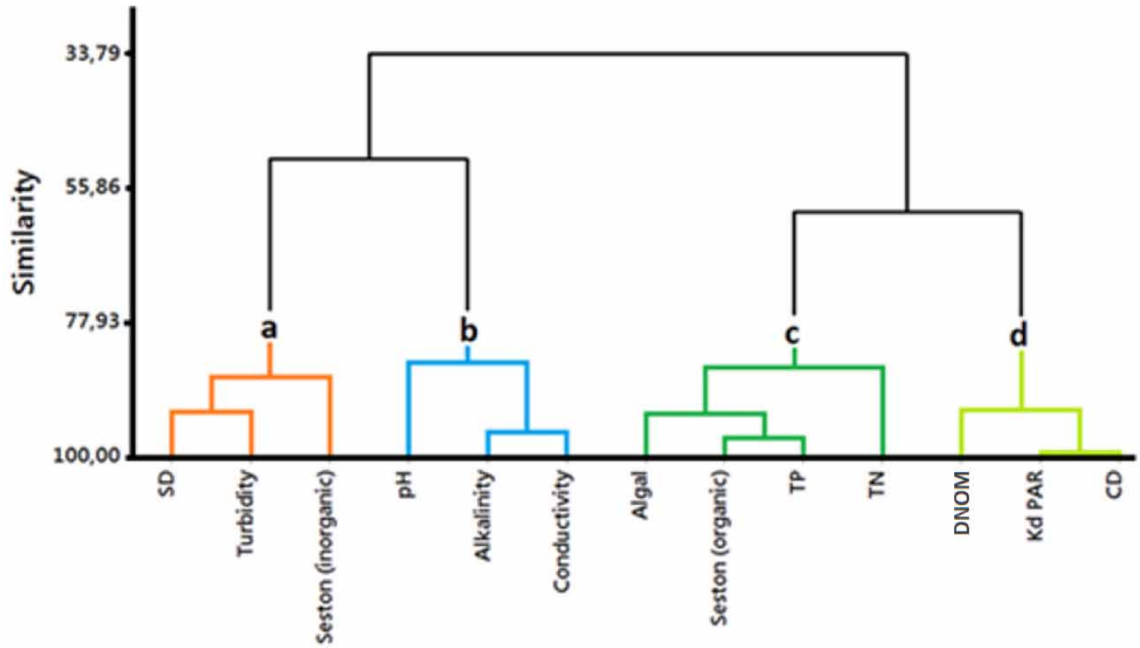

Figure 3 | Dendrogram similarity plot for correlation coefficient distance between optical parameters and water quality parameters. Seston is given in mg L^{-1}, TP and TN in μg L^{-1}, alkalinity in $mmol_c$ L^{-1}, k_d PAR, DNOM, Secchi depth (SD), and compensation depth (CD) in m^{-1}, algal (wet) in mm^3 m^{-3}, turbidity in FNU, and conductivity in mS m^{-1}. The letters (a–d) are labels of clusters of the dendrogram. The first separation represents a split into one 'inorganic' (a, b) and one 'organic/nutrient' branch (c, d; see text).

and alkalinity. Notably, shifts in the concentrations of inorganic seston are observed when transitioning from lakes situated above the marine limit (ML) to those below it. Lakes located below the ML in Southeastern Norway tend to exhibit higher levels of dissolved inorganic ions (leading to increased conductivity) and often have greater inorganic buffer capacity (alkalinity) (Haaland *et al.* 2010). The concentration of inorganic suspended matter, particularly clay particles, affects Z_{SD} and is expected to have a more pronounced impact when moving below the ML (Kirk 1985). The second branch, cluster_c, includes nutrients, algae, and the organic fraction of seston. Within this cluster, there is a strong linear correlation between the organic fraction of seston and chlorophyll (Chl_a) concentrations ($r^2 = 0.92$), as well as total algal count ($r^2 = 0.87$). This suggests a relationship between the organic matter produced within the system (e.g., algae, cyanobacteria) and the measured particulate organic matter. Additionally, cluster_d within the same branch represents the influence of organic matter originating from catchment soils on the compensation depth (Z_{CD}). It indicates that Z_{CD} is substantially affected by organic matter derived from the surrounding catchment (allochthonous-derived DNOM). The robust linear relationship observed between allochthonous DNOM and DOC, as well as between DOC and Hazen color units (TCU), further supports the significant influence of allochthonous DNOM in this study.

Figure 4 presents the loading plot for the first and second components of a principal component analysis (PCA). The PCA includes variables such as Secchi depth (Z_{SD}), compensation depth (Z_{CD}), dissolved and particulate matter, inorganic buffer capacity, and conductivity. The combined contribution of PC1 and PC2 accounts for 70% of the total variation in the dataset. Variations in Z_{SD} and Z_{CD} are well explained by changes in DNOM, turbidity, and seston along the first principal component (PC1), which represents 44% of the total variation. Both dissolved and suspended matter have an impact on the absorption and scattering of PAR-light, influencing the transparency of the water (Kirk 2011). It should be noted that DNOM is negatively correlated with PC1, while the inorganic fraction of the total seston is positively correlated with alkalinity and conductivity along the second principal component (PC2), which accounts for 26% of the total variation. This suggests that the highest concentrations of DNOM in Southeastern Norwegian lakes are typically found in forested catchments above the ML. Furthermore, the solubility of DNOM decreases with increasing ionic strength, which is somewhat associated with measurements of higher alkalinity and conductivity (De Wit *et al.* 2007; Haaland *et al.* 2010; Monteith *et al.* 2023). Below the ML, there is also an increase in suspended clay particles, which contribute to the inorganic fraction of the seston.

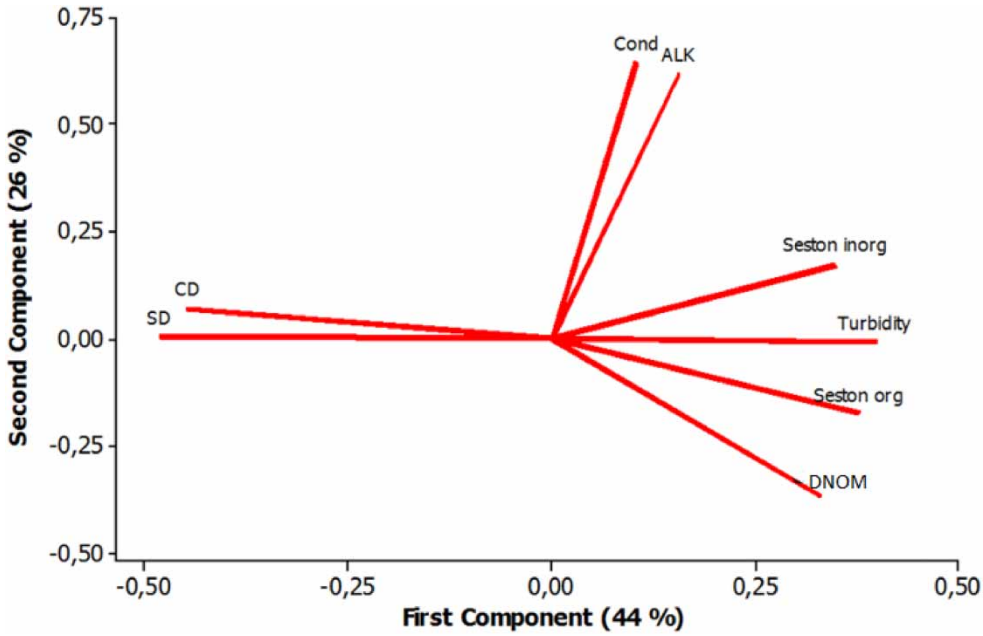

Figure 4 | PCA for integrated water-core sampled parameters and *in situ* measured optical parameters. First and second component of the PCA loading plot, containing Z_{CD} and Z_{SD}, along with dissolved and particulate matter, inorganic buffer capacity and conductivity, explains 70% of the variation in the dataset. Secchi depth (Z_{SD}) and compensation depth (Z_{SD}) data are normalized from m^{-1}, data on seston is normalized from mg L^{-1}, turbidity from FNU and conductivity from mS m^{-1}.

DISCUSSION

One uncertainty in a transfer of measurements from Z_{SD} to Z_{CD} is that Z_{SD} is interpreted by human eyes, whereas Z_{CD} is measured using digital quantum sensors. The human trichromatic color vision has a higher spectral sensitivity in the mid-PAR-spectra (Soffer & Lynch 1999; Stockman & Sharpe 2000). Compared to the human color vision, a quantum sensor instrument strives to have a relatively flat sensitivity curve throughout the whole PAR-spectrum. Hence, the human eyes might, in comparison to a quantum sensor, be somewhat less capable of detecting variations in light absorbance within the blue end of the PAR-spectra in where DNOM absorb light. To some extent, this might explain why the measurement of Z_{SD} is considerably better described by inorganic seston and turbidity than by DNOM ($r^2 = 0.74$ vs 0.25), in comparison to the respective linear correlations for Z_{CD} ($r^2 = 0.32$ vs 0.72) (Table 2). From this, Z_{CD} and Z_{SD} are influenced to a diverse degree by different processes and sources (Figures 3 and 4), such as the leaching of DNOM from catchment soils, and catchment erosion and resuspension in lakes (particles, turbidity).

Simple non-linear regression for Z_{CD}:Z_{SD} ratios using ratios between measured predictors for Z_{CD} and Z_{SD} obtained from Table 2 as model predictors are shown in Table 3. The general equation for the non-linear power trendline model is shown below:

$$\frac{Z_{CD}}{Z_{SD}} = k \cdot \left(\frac{\text{Measured predictor for } Z_{CD}}{\text{Measured predictor for } Z_{SD}}\right)^{a}$$

Table 2 | Linear regression between model predictors and compensation depth (Z_{CD}) and Secchi depth (Z_{SD})

Response parameter	Model predictor	Coeff	SE	*n*	r^2	*p*
Z_{CD} (m^{-1})	DNOM	6.81	0.92	23	0.72	<0.01
	$Seston_{org}$	5.76	1.09	23	0.57	<0.01
	Turbidity	13.3	4.19	23	0.32	<0.01
Z_{SD} (m^{-1})	$Seston_{tot}$	8.5	0.47	23	0.94	<0.01
	Turbidity	12.8	1.67	23	0.74	<0.01
	DNOM	2.56	0.97	23	0.25	<0.05

Table 3 | Non-linear regression between model predictors and the Z_{CD}:Z_{SD} ratios

Response parameter	Model predictor	*k*	*a*	r^2
Z_{CD}:Z_{SD} ratios	DNOM:Turbidity*	1.35	−0.275	0.94
	DNOM:Turbidity	1.28	−0.210	0.70
	DNOM:Seston$_{tot}$	1.24	−0.220	0.60
	DNOM:Seston$_{org}$	1.36	−0.136	0.20

The non-linear power trendline for Z_{CD}:Z_{SD} ratio is given by k*(model predictor)^a. The DNOM:Turbidity* model predictor incorporates lakes with a seston$_{org}$ to seston$_{inorg}$ ratio > 5 (5 of 23 lakes have been excluded). This was done to emphasize the scattering capability and lessen the absorption facility of the suspended autochthonous produced organic matter measured as turbidity.

The best set of model predictors for Z_{CD}:Z_{SD} ratios were found to be the DNOM:turbidity ratios (Table 3) and its explained variance ($r^2 = 0.70$) was similar to findings in shallow coastal waters by Luhtala & Tolvanen (2013). To focus more specifically on processes and catchment drivers, it is appropriate to differentiate between DNOM and turbidity derived from organic sources (Seston$_{org}$) originating from autochthonous production within the lakes and allochthonous sources. Hence, by excluding lakes with a Seston$_{org}$:Seston$_{inorg}$ ratio > 5 (five lakes excluded), the simple non-linear regression model explains 94% of the variation in the Z_{CD}:Z_{SD} ratios among the lakes (Table 3 and Figure 5).

While some lakes in Norway have undergone less dramatic changes in DNOM concentrations, there has been a notable and statistically significant positive trend within the lake district and throughout a larger portion of Southern Norway (Monteith *et al.* 2007, 2023; Grennfelt *et al.* 2020). There has however not been a similar trend for turbidity (Haaland

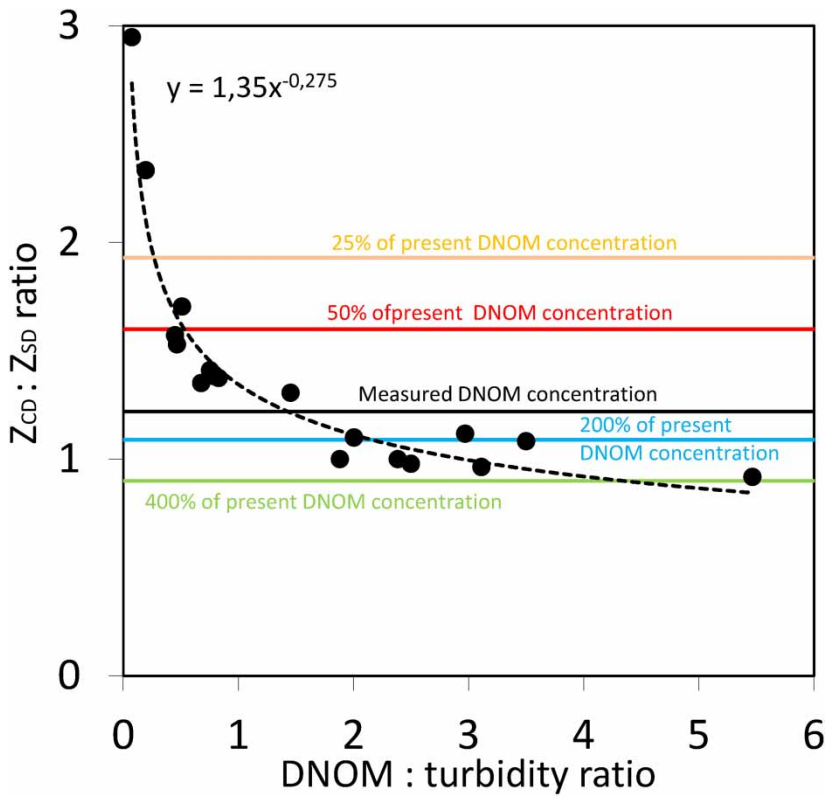

Figure 5 | Z_{CD}:Z_{SD} ratio plotted against the ratio between DNOM (400 nm) and turbidity (NTU). Measured data is shown as black dots. The median values of the measured Z_{CD}:Z_{SD} ratios are shown as a black solid line. Median values for calculated Z_{CD}:Z_{SD} ratios for the lake district for 25, 50, 200, and 400% of the current DNOM concentrations are shown as an orange, a red, a blue, and a green solid line, respectively. *Note*: Lakes in the survey with a seston$_{org}$:seston$_{inorg}$ ratio > 5 have been excluded from the model (5 of 23 lakes; see text and Table 1). Please refer to the online version of this paper to see this figure in colour: https://dx.doi.org/10.2166/wcc.2023.217.

et al. 2010; Riise *et al.* 2018). Extensive ongoing monitoring networks in Norway on climate, atmospheric composition, and atmospheric deposition (Aas *et al.* 2022) have been used to identify parameters explaining the DNOM development in the lake district, of which acid rain and climate parameters such as air temperature and precipitation amount and intensity are important drivers (Haaland *et al.* 2006, 2010; De Wit *et al.* 2016; Monteith *et al.* 2023). Currently, sulfate emissions in Europe are low and comparable to levels recorded in the late 1890s or early 1900s (Grennfelt *et al.* 2020). Since the mid-1980s, acid deposition over the lake district has subsequently experienced a significant decrease (Riise *et al.* 2023). Furthermore, both air temperature and precipitation amount, and also numbers of episodes with high precipitation intensity, have increased over the previous decades in the lake district (Kuya *et al.* 2023). By employing even a moderately conservative scenario from the IPCC (Intergovernmental Panel on Climate Change; RCP4.5; stable/slightly increasing emissions until 2040; then reduced emissions), climate projections for the lake district still indicate higher temperatures and more rainfall in the lake district up until the year 2100 (Hanssen-Bauer *et al.* 2017; uncertainties in the climate projections related to future anthropogenic emissions, natural climate variations and variations between different climate models have here been taken into account). By incorporating the previous DNOM concentrations during the acid rain peak period in the mid-1980s and 1990s, and also the anticipated higher future DNOM concentrations due to climate change in the lake district, it is from our findings possible to give an estimate of both previous and expected future Z_{CD}:Z_{SD} ratios for the lakes within the lake district. During the peak acid rain period, DNOM concentrations were notably lower compared to present levels (Haaland *et al.* 2010). Compared to the present, DNOM concentrations were often just half or even just a quarter of the current concentration, and from that the median Z_{CD}:Z_{SD} ratios are estimated to have been approximately 30 and 60% higher than today, respectively (Figure 5). The Z_{CD}:Z_{SD} ratios within lakes are expected to change somewhat from day to day, and throughout the year as a result of natural weather fluctuations, seasonal variations, and variations in inputs of parameters influencing light absorbance and light scattering. However, apart from these expected short-term fluctuations, our findings hence indicate that the Z_{CD}:Z_{SD} ratios also have experienced a strong *long-term* decline in the lake district over the past few decades. Moreover, a further climate-driven increase in DNOM concentrations, that is expected to occur due to increased temperature and increased precipitation inside the lake district (Haaland *et al.* 2010; De Wit *et al.* 2016; Hanssen-Bauer *et al.* 2017), median Z_{CD}:Z_{SD} ratios in the lake district are estimated to further decline with approximately 10 and 25% compared to current levels if there were to be a doubling or quadrupling in the DNOM concentrations, respectively (Figure 5).

CONCLUSION

Two commonly employed light irradiance measurements in lakes are the Secchi depth (Z_{SD}) and the compensation depth (Z_{CD}). The Z_{CD}:Z_{SD} ratios in a lake district located in Southeastern Norway are estimated to have experienced a significant long-term decrease. The decrease can be attributed to a diverse influence of DNOM on these light irradiance measurements, in combination with long-term increasing concentrations of DNOM. As climate change continues to impact DNOM concentrations in the region, this trend is expected to persist. The Z_{CD}:Z_{SD} ratio in these lakes might hence be less stable than we have expected, and when estimating Z_{CD} using Z_{SD} measurements, one should be aware of this possible long-term change. Although our current set-up with water-core samples allows us to identify this issue, it is required to conduct additional research in both *in situ* and laboratory settings to address this topic in more detail.

ACKNOWLEDGEMENTS

Our deepest gratitude to late Assoc Prof Inggard Arne Blakar (Norwegian University of Life Sciences, NMBU) for valuable inputs on the topic and the *in situ* water-core sampling procedure.

DATA AVAILABILITY STATEMENT

All relevant data are included in the paper or its Supplementary Information.

CONFLICT OF INTEREST

The authors declare there is no conflict.

REFERENCES

Aas, W., Bohlin-Nizzetto, P., Hak, C., Aspmo Pfaffhuber, K. & Uggerud, H. 2022 *Monitoring Atmospheric Composition and Deposition in Norway*. Norwegian Institute for Air Research (NILU) Report 7/2022. ISBN: 978-82-425-3076-9. hdl.handle.net/11250/2987017.

Bohren, C. F. & Huffman, D. R. 1998 *Absorption and Scattering of Light by Small Particles*. John Wiley & Sons, Inc. https://doi.org/10.1002/9783527618156.

Branco, A. B. & Kremer, J. N. 2005 The relative importance of chlorophyll and colored dissolved organic matter (CDOM) to the prediction of the diffuse attenuation coefficient in shallow estuaries. *Estuaries* **28**, 643–652.

Brezonic, P. L. 1978 Effects of organic color and turbidity on Secchi disk transparency. *Journal of the Fisheries Research Board of Canada* **35**, 1410–1416.

Clark, J. M., Chapman, P. J., Heatwaite, A. L. & Adamson, J. K. 2006 Suppression of dissolved organic carbon by sulfate induced acidification during simulated droughts. *Environmental Science & Technology* **40**, 1776–1783.

De Wit, H. A., Mulder, J., Hindar, A. & Hole, L. 2007 Long-term increase in dissolved organic carbon in streamwaters in Norway is response to reduced acid deposition. *Environmental Science & Technology* **41**, 7706–7713.

De Wit, H. A., Valinia, S., Weyhenmeyer, G. A., Futter, M. N., Kortelainen, P., Austnes, K., Hessen, D., Raike, A., Laudon, H. & Vournenmaa, J. 2016 Current browning of surface waters will be further promoted by wetter climate. *Environmental Science & Technology* **3** (12), 430–435.

De Wit, H. A., Garmo, Ø. A., Jackson-Blake, L. A., Clayer, F., Vogt, R. D., Austnes, K., Kaste, Ø., Gundersen, C. B., Guerrerro, J. L. & Hindar, A. 2023 Changing water chemistry in one thousand Norwegian lakes during three decades of cleaner air and climate change. *Global Biogeochemical Cycles* **37**. ISSN 0886-6236. doi:10.1029/2022GB007509.

Eloranta, P. 1978 Light penetration in different types of lakes in Central Finland. *Holarctic Ecology* **1**, 362–366.

Evans, C. D., Chapman, P. J., Clark, J. M., Monteith, D. T. & Cresser, M. S. 2006 Alternative explanations for rising dissolved organic carbon export from organic soils. *Global Change Biology* **12**, 2044–2053.

Finstad, A. G., Andersen, T., Larsen, S., Tominaga, K., Blumentrath, S., De Wit, H. A., Tømmervik, H. & Hessen, D. O. 2016 From greening to browning: catchment vegetation development and reduced S-deposition promote organic carbon load on decadal time scales in Nordic lakes. *Scientific Reports* **6**, 31944. doi:10.1038/srep31944.

Forsberg, C. & Petersen, R. C. 1990 A darkening of Swedish lakes due to increased humus inputs during the last 15 years. *Verhandlungen des Internationalen Verein Limnologie* **24**, 289–292.

Freeman, C., Evans, C. D. & Monteith, D. T. 2001 Export of organic carbon from peat soils. *Nature* **412**, 785.

Gjessing, E. 1964 Ferrous iron in water. *Limnology and Oceanography* **9** (2), 272–274. doi:10.4319/lo.1964.9.2.0272.

Grennfelt, P., Engleryd, A., Forsius, M., Hov, Ø., Rodhe, H. & Cowling, E. 2020 Acid rain and air pollution: 50 years of progress in environmental science and policy. *Ambio* **49** (4), 849–864. doi:10.1007/s13280-019-01244-4.

Haaland, S., Riise, G. & Stuanes, A. O. 2006 The impact of precipitation on the quality of dissolved organic carbon in runoff from a headwater area in Norway. *Verhandlungen des Internationalen Verein Limnologie* **29** (5), 2317–2321.

Haaland, S., Riise, G., Hongve, D., Laudon, H. & Vogt, R. D. 2010 Quantifying the drivers of increasing colored organic matter in boreal surface waters. *Environmental Science & Technology* **44** (8), 2975–2980. doi:10.1021/es903179j.

Haaland, S., Eikebrokk, B., Riise, G. & Vogt, R. 2018 Future browning of Western Scotland raw waters. In: *Poster. The 11th Nordic Drinking Water Conference*, 11–13 June, Oslo. doi:10.13140/RG.2.2.32084.71047.

Hanssen-Bauer, I., Førland, E. J., Haddeland, I., Hisdal, H., Lawrence, D., Mayer, D., Nesje, A., Nilsen, J. E. Ø., Sandven, S., Sandø, A. B., Sorteberg, A. & Ådlandsvik, B. 2017 *Climate in Norway 2100 – A Knowledge Base for Climate Adaptation. Report 1/2017*. ISSN 2387-3027. Norwegian Centre for Climate Services.

Hytteborn, J. K., Temnerud, J., Alexander, R. B., Boyer, E. W., Futter, M. N., Fröberg, M., Dahné, J. & Bishop, K. H. 2015 Patterns and predictability in the intra-annual organic carbon variability across the boreal and hemi-boreal landscape. *Science of the Total Environment* **520**, 260–269. doi.org/10.1016/j.scitotenv.2015.03.041.

Kirk, J. T. O. 1976 Yellow substance (gelbstoff) and its contribution to the attenuation of photosynthetically active radiation in some inland and coastal south-eastern Australian waters. *Australian Journal of Marine and Freshwater Research* **27**, 61–71.

Kirk, J. T. O. 1980 Spectral absorption properties of natural waters: contribution of the soluble and particulate fractions to light absorption in some inland waters of south-east Australia. *Australian Journal of Marine and Freshwater Research* **3**, 287–296.

Kirk, J. T. O. 1985 Effects of suspensoids (turbidity) on penetration of solar radiation in aquatic ecosystems. *Hydrobiologia* **125**, 195–208.

Kirk, J. T. O. 2011 *Light and Photosynthesis in Aquatic Ecosystems*, 3rd edn. Cambridge University Press, Cambridge.

Koenings, J. P. & Edmundson, J. A. 1991 Secchi disk and photometer estimates of light regimes in Alaskan lakes: Effects of yellow color and turbidity *LimnolOceanogr* **36**, 91–105.

Kostoglidis, A., Pattiaratchi, C. B. & Hamilton, D. P. 2005 CDOM and its contribution to the underwater light climate of a shallow, microtidal estuary in south-western Australia. *Estuarine, Coastal and Shelf Science* **63**, 469–477.

Kritzberg, E. S. & Ekström, S. M. 2012 Increasing iron concentrations in surface waters – a factor behind brownification? *Biogeosciences* **9**, 1465–1478. doi:10.5194/bg-9-1465-2012.

Kuya, E. K., Hanssen-Bauer, I., Mayer, S. & Heiberg, H. 2023 *Rain, Sleet and Snow in Norway 1971-2000: Observations Vs. Results From Climate Models. Report 1/2023*. ISSN 2704-1018. Norwegian Centre for Climate Services.

Larsen, S., Andersen, T. & Hessen, D. O. 2010 Climate change predicted to cause severe increase of organic carbon in lakes. *Global Change Biology* **17** (2), 1186–1192. doi:10.1111/j.1365-2486.2010.02257.x.

Luhtala, H. & Tolvanen, H. 2013 Optimizing the use of Secchi depth as a proxy for euphotic depth in coastal waters: an empirical study from the Baltic Sea. *ISPRS International Journal of Geo-Information* **2**, 1153–1168. doi:10.3390/ijgi2041153.

Monteith, D. T., Stoddard, J. L., Evans, C. D., De Wit, H. A., Forsius, M., Høgåsen, T., Wilander, A., Skjelkvåle, B. L., Jeffries, D. S., Vuorenmaa, J., Keller, B., Kopaćek, J. & Vesely, J. 2007 Dissolved organic carbon trends resulting from changes in atmospheric deposition chemistry. *Nature* **450**, 537–541.

Monteith, D. T., Henrys, P. A., Hruska, J., De Wit, H. A., Kram, P., Moldan, F., Posch, M., Raike, A., Stoddard, J. L., Shilland, E. M., Pereira, M. G. & Evans, C. D. 2023 Long-term rise in riverine dissolved organic carbon concentration is predicted by electrolyte solubility theory. *Science Advances* **9** (3). doi:10.1126/sciadv.ade3491.

Poulin, B. A., Ryan, J. N. & Aiken, G. R. 2014 Effects of iron on optical properties of dissolved organic matter. *Environmental Science & Technology* **48** (17), 10098–10106. doi:10.1021/es502670r.

Preisendorfer, R. W. 1986 Secchi disk science: visual optics of natural waters. *Limnology and Oceanography* **31** (5), 909–926.

Read, J. S. & Rose, K. C. 2013 Physical responses of small temperate lakes to variation in dissolved organic carbon concentrations. *Limnology and Oceanography* **58** (3), 921–931. doi:10.4319/lo.2013.58.3.0921.

Riise, G., Müller, R. A., Haaland, S. & Wehenmeyer, G. A. 2018 Acid rain – a strong external driver that has suppressed water colour variability between lakes. *Boreal Environment Research* **23**, 69–81.

Riise, G., Haaland, S. & Xiao, Y. 2023 Coupling of iron and dissolved organic matter in lakes – selective retention of different size fractions. *Aquatic Sciences* **85**, 57.

Rohrlack, T., Frostad, P., Riise, G. & Hagman, C. H. C. 2020 Motile phytoplankton species such as *Gonyostomum semen* can significantly reduce CO_2 emissions from boreal lakes. *Limnologica* **84**. https://doi.org/10.1016/j.limno.2020.125810.

Shapiro, J. 1957 Chemical and biological studies on the yellow organic acids of lake water. *Limnology and Oceanography* **2**, 161–179.

Simon, A. & Shanmugam, P. 2013 A new model for the vertical spectral diffuse attenuation coefficient of downwelling irradiance in turbid coastal waters: validation with in situ measurements. *Optics Express* **21** (24), 30082–30106. doi:10.1364/OE.21.030082.

Smetacek, V. & Passow, U. 1990 Spring bloom initiation and Sverdrup's critical-depth model. *Limnology and Oceanography* **35** (l), 228–234.

Soffer, B. H. & Lynch, D. K. 1999 Some paradoxes, errors, and resolutions concerning the spectral optimization of human vision. *American Journal of Physics* **67** (11), 946–953.

Steinberg, C. E. W. 2003 *Ecology of Humic Substances in Freshwaters*. Springer, Berlin.

Stockman, A. & Sharpe, L. T. 2000 The spectral sensitivities of the middle- and long-wavelength-sensitive cones derived from measurements in observers of known genotype. *Vision Research* **40** (13), 1711–1737. doi:10.1016/S0042-6989(00)00021-3.

Thrane, J. E., Hessen, D. O. & Andersen, T. 2014 The absorption of light in lakes: negative impact on dissolved organic carbon on primary productivity. *Ecosystems*. doi:10.1007/s10021-014-9776-2.

Urtizberea, A., Dupont, N., Rosland, R. & Aksnes, D. L. 2013 Sensitivity of euphotic zone properties to CDOM variations in marine ecosystem models. *Ecological Modelling* **256**, 16–22.

Van Sickle, J. 1997 Using mean similarity dendrograms to evaluate classifications. *Journal of Agricultural, Biological and Environmental Statistics* **2**, 370–388.

Weyhenmeyer, G. A., Prairie, Y. T. & Tranvik, L. J. 2014 Browning of boreal freshwaters coupled to carbon-iron interactions along the aquatic continuum. *PLoS ONE* **9** (2), e88104. doi:10.1371/journal.pone.0088104.

First received 27 April 2023; accepted in revised form 15 July 2023. Available online 31 July 2023